Receding-Horizon Multi-Objective Optimization for Disaster Response

Kooktae Lee, Sonia Martínez, Jorge Cortés, Robert H. Chen, and Mark B. Milam

Abstract— **This paper proposes a receding-horizon, multi-objective optimization approach for robot motion planning in disaster response scenarios. During a search and rescue mission, a robot is deployed in the disaster area to find and egress all victims. In doing so, multiple criteria characterize the effectiveness of such plan. We define three objective functions (performance, uncertainty about victim locations, and uncertainty about the environment) and formulate a multi-objective optimization problem employing a combined weighted-sum and ϵ-constraint method. To handle dynamic scenarios, we employ a receding-horizon approach that allows to dynamically adapt the ϵ constraint. We illustrate the effectiveness of the proposed method via simulations.**

I. INTRODUCTION

The adequate use of limited robotic resources in search and rescue missions is of critical importance. Generally, disaster areas tend to be spatially large and hence an efficient plan to find and rescue all victims in a limited amount of time is necessary. While robots equipped with several onboard sensors are capable of either exploring, finding, or servicing victims individually, efficiency requires high-level strategies that can determine how to alternate among these tasks in an effective manner. Depending on the context, some of these objectives may be aligned or in conflict, which leads to the question of how to find adaptive policies that exploit synergies between different objectives at different times. Motivated by this, here we propose a method that builds on multi-objective optimization tools to capture these tradeoffs.

Literature Review: In [1], an algorithm is proposed for a distributed team of autonomous mobile robots to search for an object. This method can be implemented in a fully distributed manner during the search stage and then, during the rescue stage, cooperative is carried out via communications between distributed robots. A case study for human-robot interaction in the urban search and rescue task is evaluated in [2], based on the World Trade Center rescue response. An unmanned aircraft system design for urban search and rescue missions is presented in [3], where several sensors are used for indoor and outdoor navigation with a fusion technique using the extended Kalman filter. The work [4] integrates target search and tracking methods for multiple fixed-wing unmanned air vehicles, and develops a high-level control logic based on finite state automaton mode. While the above studies are related to action plans in disaster response

scenarios, many results have been developed as a methodology for coverage path planning; see also [5]. Coverage path planning is closely related to the design of a path for the purpose of covering areas of interest. Examples of this approach include lawn mowers [6], [7], cleaning robots [8], autonomous underwater vehicles [9], aerial remote sensing in agriculture [10], and automated harvesting [11]. According to [12], heuristic algorithms may work well in extended simulations without providing theoretical guarantees on the coverage performance, while provably correct algorithms usually require more computational power or time to complete. As a tool to capture tradeoffs in routing problems for disaster relief operations, multi-objective optimization approaches [13]–[15] have been adopted to applications such as emergency supply path optimization [16], [17], multi-period emergency logistics [18], rout choice of humanitarian response planning for disaster response [19], optimal evacuation planning [20], [21]. However, these approaches assume that locations for both rescuers and evacuees are known a priori. Other works [22], [23] provide solutions to the motion planning and control problem for multiple robots by adopting a receding horizon approach. In spite of these contributions to strategic action plans for disaster response, efficient strategies that account for multiple criteria simultaneously are still lacking.

Statement of Contributions: We formulate a multi-objective optimization problem whose solution provides an optimized trajectory to realize an efficient high-level strategy in disaster response scenarios. The objective functions in the multi-objective optimization problem are defined by the robot performance, uncertainty about the detected victims' location, and uncertainty about the environment. To solve this three-function multi-objective optimization problem, we propose a method that combines the classical weighted-sum and ϵ-constraint methods in a receding horizon fashion that incorporates measurement updates provided by the robot at each time step of the plan. Based on the analysis of the optimal trajectories for the cost function, we determine the minimum value of the associated ϵ, and translate the decision maker's choice into an easier-to-tune parameter. We further exploit this result to adapt dynamically the value of the constraint in our receding-horizon algorithm, aiming for less conservativeness. We illustrate the proposed method in a simulation scenario. For reasons of space, the proofs of all results are omitted and will appear elsewhere.

Notation: The set of real and natural numbers are $\mathbb{R}$ and $\mathbb{N}$, respectively. Further, $\mathbb{N}_0 = \mathbb{N} \cup \{0\}$. The symbol $\mathrm{tr}(\cdot)$ and $\|\cdot\|$ denotes the trace and Euclidean norm, respectively. The symbols $\det(\cdot)$ and $\mathrm{adj}(\cdot)$ denote, respectively, the determinant and adjoint of a matrix. Expectation with respect to a

given probability is $\mathbb{E}[\cdot]$. Finally, $\mathcal{N}(\mu, \Sigma)$ denotes a Gaussian probability density function with mean μ and covariance Σ.

II. PROBLEM DESCRIPTION

In our disaster-response scenario, the major tasks are to find all victims and rescue all survivors by one robot. Throughout the paper, we assume that *the robot is able to complete its tasks (e.g., service and rescue) for each victim when the robot arrives at the victim location.* At time $t \in \mathbb{N}_0$, the location of the robot and the victim are, respectively, denoted by $x_t \in \mathbb{R}^2$ and $\theta_t \in \mathbb{R}^2$. We assume that victims are stationary and thus, their locations are fixed.

A. Formulation of Multiple Objective Functions

Our approach to the robot motion planning problem is to solve a multi-objective optimization problem of the form,

$$\underset{x}{\text{minimize}} \quad [F_1(x), F_2(x), \ldots, F_n(x)]$$
$$\text{subject to} \quad x \in X,$$

where a point $x^\star \in X$ is said to Pareto optimal if and only if there does not exist another point $x \in X$, such that $F_i(x) \leq F_i(x^\star), \forall i \in \{1, 2, \ldots, n\}$ and $F_j(x) \leq F_j(x^\star)$ for at least one index $j \in \{1, 2, \ldots, n\}$.

The main objective functions considered in our scenario are determined by the following functions depending on a decision variable $x = [x_1^T, x_2^T, \ldots]^T$, representing the trajectory of the robot.

- $f_1(x, \theta_t)$: the robot performance, which we measure by the distance between the robot and the victim;
- $f_2(x, \theta_t)$: uncertainty about the location of the victim, caused by the measurement noise;
- $f_3(x)$: uncertainty about an unknown environment including the number of victims and the approximate location of them.

Although f_2 and f_3 represent uncertainty, they are different from each other in the following sense. Before the robot explores the disaster area, the robot does not know how many victims there are as well as where they are located. Therefore, this uncertainty over the domain is quantified by some metric, which will be related to f_3. On the other hand, after the robot has detected a victim by onboard sensors, there is still uncertainty on where it is caused by the sensor measurement inaccuracy. In this case, the straight path connecting two points between the current location of the robot and the expected location of the victim may not be desirable to get to the victim. This quantity is thus represented by f_2.

B. Robot Measurement Model

The sensor attached to the robot provides information about the victim location. No underlying assumptions are placed on the specific type (technology) of sensors, however, we consider that the sensor can provide range measurements such as sonar, infrared, ultrasonic, and laser sensors. Since these sensors have the limited sensing range, the robot needs to explore the disaster area in order to find all victims.
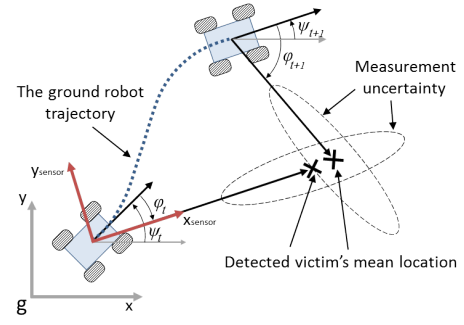

Fig. 1: An illustration of a ground robot, its trajectory and a victim location. Sensor uncertainty is shown by means of confidence ellipses at different measurement times.

The measurement model of the sensor is given as follows:

$$z_t = \Upsilon(x_t, \theta_t) + \omega_t,$$

where $z_t \in \mathbb{R}^2$ is the observation vector representing the victim location at time $t \in \mathbb{N}_0$, $\Upsilon(x_t, \theta_t)$ is the measurement function in terms of the current location of the robot x_t and the victim θ_t, and ω_t is the white noise with zero mean and covariance $\Sigma_t^{\text{obs}} \in \mathbb{R}^{2 \times 2}$ given by

$$\Sigma_t^{\text{obs}} = \begin{bmatrix} \sigma_x^2 & 0 \\ 0 & \sigma_y^2 \end{bmatrix}, \tag{1}$$

where σ_x and σ_y to represent the standard deviation along the local frame of the sensor (x_{sensor} and y_{sensor} in Fig. 1). We assume that $\sigma_x > \sigma_y$ for the sensor model (i.e., uncertainty along x_{sensor} is larger than that along y_{sensor}).

In a global coordinate frame (denoted by the left superscript g in the symbol), the mean location of the victim is obtained by $^g\mu_t^{\text{obs}} = \mu_t^{\text{obs}} + x_t$, where $\mu_t^{\text{obs}} = \mathbb{E}[z_t]$, x_t is the current (exactly known) position of the robot.

The covariance matrix for victim location is transformed by using a rotation matrix $\mathbf{R}(\beta)$ into

$$^g\Sigma_t^{\text{obs}} = \mathbf{R}(\beta_t)^T \Sigma_t^{\text{obs}} \mathbf{R}(\beta_t), \tag{2}$$

where $\mathbf{R}(\beta_t)$ and the angle β_t are given by

$$\mathbf{R}(\beta_t) = \begin{bmatrix} \cos(\beta_t) & -\sin(\beta_t) \\ \sin(\beta_t) & \cos(\beta_t) \end{bmatrix}, \quad \beta_t = (\psi_t + \varphi_t).$$

with ψ_t and φ_t defined in Fig. 1. Whenever the robot receives a new measurement $^g\mu_{t+1}^{\text{obs}}$ and $^g\Sigma_{t+1}^{\text{obs}}$ at time $t+1$, the victim location associated with the previous value $^g\mu_t$ and $^g\Sigma_t$ is updated according to

$$^g\mu_{t+1} = {}^g\mu_t + {}^g\Sigma_t({}^g\Sigma_t + {}^g\Sigma_{t+1}^{\text{obs}})^{-1}({}^g\mu_{t+1}^{\text{obs}} - {}^g\mu_t),$$
$$^g\Sigma_{t+1} = {}^g\Sigma_t - {}^g\Sigma_t ({}^g\Sigma_t + {}^g\Sigma_{t+1}^{\text{obs}})^{-1} {}^g\Sigma_t. \tag{3}$$

With this measurement and update model, we formulate the multi-objective optimization problem for disaster response scenarios in the following section.

III. MULTI-OBJECTIVE OPTIMIZATION OVER A FINITE-TIME HORIZON

The future trajectory of the robot $\{x_{t+1}, x_{t+2}, \ldots, x_{t+h}\}$ can be obtained by solving a multi-objective optimization

problem with an infinite horizon length h. However, the gains in modeling accuracy of the infinite-horizon problem are severely compromised by its technical difficulties: 1) the parameters are not known exactly, and vary in time (even if victims do no move, the uncertainty on parameter θ_t changes over time with new sensor observations); 2) for large horizon lengths h, computational issues arise.

To avoid these concerns, we use the receding horizon framework. At the current time t, only a small horizon h will be considered to predict the trajectory of the robot with the current estimate for θ_t, and the robot moves to the very first step of the planned trajectory. If a new measurement is available, then the robot updates θ_t and generates a new trajectory. In the following, we present a particular multi-objective optimization formulation that is employed with receding horizon control approach.

Consider the multi-objective optimization problem associated with the finite-time horizon h as follows.

$$\underset{x_{t+1,\ldots,t+h}}{\text{minimize}} \quad [F_1(x_{t+1:t+h}|\theta_t),\ F_2(x_{t+1:t+h}|\theta_t),\ F_3(x_{t+1:t+h})]$$

$$\text{subject to} \quad g_i(x_{t+1:t+h}) \le 0,\ i = 1,\ldots,m,$$
$$h_j(x_{t+1:t+h}) = 0,\ j = 1,\ldots,n,$$
$$(4)$$

where $x_{t+1:t+h} := [x_{t+1}^T, x_{t+2}^T, \ldots, x_{t+h}^T]^T \in \mathbb{R}^{2h}$ is a concatenated decision vector describing the trajectory of the robot from time $t+1$ to $t+h$. Robot dynamic constraints are represented by $g_i(x_{t+1:t+h})$ and $h_j(x_{t+1:t+h})$, respectively. For instance, there may exist an upper bound in the moving distance of the robot at each time step due to a limit in the velocity of the robot.

A. Objective Function for Quantifying Performance

For each detected victim $\theta_t^j \sim \mathcal{N}(^g\mu_t^j, {}^g\Sigma_t^j)$, the performance measure f_1^j is defined by

$$f_1^j(x_{t+1:t+h}|\theta_t^j) := \min_{i \in \{t+1,\ldots,t+h\}} \{\|x_i - {}^g\mu_t^j\|\}, \quad (5)$$

where $^g\mu_t^j$ describes the mean location of θ_t^j at time t. This objective function describes the minimum distance between the robot trajectory and the mean location of the victim. Since we are considering multiple victims detected at the same time, the priority for visiting multiple candidate locations needs to be established. This priority must reflect both uncertainty about the victim location as well as proximity of the robot to the victim. Thus, F_1 is defined by

$$F_1(x_{t+1:t+h}|\theta_t) = \{f_1^{j^\star}|j^\star = \underset{j}{\text{argmin}}\{\text{tr}({}^g\Sigma_t^j) \cdot \|x_t - {}^g\mu_t^j\|\}\}.$$

In this way, the minimization of F_1 provides the trajectory of the robot to reach the victim location that is closer and more certain.

B. Objective Function for Quantifying Uncertainty About the Victim Locations

For the given uncertainty $^g\Sigma_t^j$ about the location of the victim j, each f_2^j is defined as follows:

$$f_2^j(x_{t+1:t+h}|\theta_t^j) := \text{tr}({}^g\Sigma_{t+h}^j). \quad (6)$$

The optimal solution of the above function will be a robot trajectory $x_{t+1},\ldots,x_{t+h}$ that minimizes the term $\text{tr}({}^g\Sigma_{t+h}^j)$. Then, the F_2 function is given as an average of the multiple uncertainty terms as

$$F_2(x_{t+1:t+h}|\theta_t) = \frac{1}{N}\sum_{j=1}^{N} f_2^j(x_{t+1:t+h}|\theta_t^j), \quad (7)$$

where N is the total number of victims currently detected. A reason for taking an average of different f_2^j is that the motion of the robot will minimize the uncertainties about all victims' location in a balanced way. A possible concern about the F_2 definition above is that the optimal solution that minimizes F_2 may increase some of f_2^j even if their average F_2 decreases. We show that this is not the case in the following result. The proof is an immediate consequence of (3).

Lemma 3.1: The function f_2^j is a monotonically decreasing function with respect to the number of travel steps.

C. Objective Function for Quantifying Uncertainty About the Environment

The last objective function is defined to explore unknown areas. For this purpose, we employ the ergodic metric in [24] as follows. The distribution of possible victim locations is described by the probability density function $\rho(x)$. The ergodic metric measures to what extent the fraction of time spent by the trajectory is equal to the spatial distribution. We employ this metric in order to define our function F_3. To this end, recall that the Fourier basis function $\Gamma_k(x)$ is

$$\Gamma_k(x) = \frac{1}{h_k}\cos(k_x \mathsf{x})\cos(k_y \mathsf{y}),\ x = [\mathsf{x}, \mathsf{y}]^T,$$

where h_k is a normalizing factor, k_x and k_y are coefficients as in [24]. Then, the ergodic metric $\phi(t)$ is defined as

$$\phi(t) = \sum_{k=0}^{K} \Lambda_k |c_k(t) - \rho_k|^2, \quad (8)$$

where K is the number of the Fourier basis functions and

$$\Lambda_k = \frac{1}{(1 + \|k\|^2)^{\frac{(n+1)}{2}}},\ \text{(for 2D map, } n = 2)$$

$$c_k(t) = \frac{1}{t+1}\sum_{i=0}^{t} \Gamma_k(x_i), \quad \rho_k = \int_X \rho(x)\Gamma_k(x)dx. \quad (9)$$

Notice that $c_k(t)$ term in the above equation describes the time averages of the Fourier basis functions for the time interval $[0, t]$, where t is the current time. Then, we aim to generate the future trajectory of the robot $x_{t+1:t+h}$ by defining our objective function F_3 as

$$F_3(x_{t+1:t+h}) = \phi(t+h) = \sum_{k=0}^{K} \Lambda_k |c_k(t+h) - \rho_k|^2. \quad (10)$$

In this way, the solution of an optimization problem with the above function F_3 over a set of points $x_{t+1:t+h}$ is the trajectory $\{x_{t+1}, \ldots, x_{t+h}\}$ that minimizes the gap between the time averages of the Fourier basis functions along the trajectory (c_k) and their spatial averages with respect to the distribution (ρ_k).

IV. Algorithmic Approach

We propose a mixed method that builds on two classical approaches, the weighted-sum and ϵ-constraint methods, to multi-objective optimization problems. In particular, consider

$$
\begin{aligned}
\underset{x_{t+1:t+h}}{\text{minimize}} \quad & \alpha F_1(x_{t+1:t+h}|\theta_t) + (1-\alpha)F_3(x_{t+1:t+h}) \\
\text{subject to} \quad & \alpha F_2(x_{t+1:t+h}|\theta_t) \leq \epsilon(t+h), \\
& \|x_{i+1} - x_i\| \leq r, \quad i = t, \ldots, t+h-1,
\end{aligned}
\tag{11}
$$

where α is a positive weight representing the relative importance between the exploration (F_3) and the exploitation (F_1), and ϵ is the upper bound of uncertainty about the location of victims (F_2). The last inequality constraints denote an ℓ_2-ball characterizing the maximum moving distance of the robot at each step. The decision maker can then vary the constants α and ϵ in order to obtain a Pareto optimal solution that represents a certain tradeoff.

Our particular problem formulation is based on the following considerations. While a weighted-sum method is the simplest and most widely used method, any choice of constants do not necessarily guarantee the recovery of the full Pareto optimal front in non-convex problems. On the other hand, the ϵ constraint method provides such guarantee for any type of problem by varying the ϵ constraint parameters adequately. However, this leads to the difficulty of choosing ϵ values that lead to feasible problems and that are non-conservative at the same time. In this paper we take a middle ground approach by considering only one such ϵ constraint and studying the feasibility of the associated problem.

Due to the dynamic characteristics of the problem (i.e., time dependency of the problem associated with new sensor measurements at every time step), it is not adequate to solve (11) as a static optimization problem or as an infinite horizon problem, thus we choose a dynamic receding-horizon approach. Other critical factors in solving (11) are how to decide ϵ and α values, which may be changed dynamically at every time step. In what follows we consider a solution to the problem that modifies the ϵ constraint dynamically.

A. Dynamic ϵ-constraint method

The solution to the previous multi-objective optimization problem depends critically on the choice of parameters and, in particular, the value of ϵ. In this way, if ϵ is too small, then the problem may not be feasible. On the other hand, if the ϵ value was too large, the solution would be in favor of one objective function (F_1 in our case). In addition, the optimization problem (11) is time varying, implying that ϵ value can be changed at different times t. In the following result, we find what is the minimum value of the function F_2, which sets a lower bound on the value of ϵ that makes the multi-objective optimization problem feasible. Based on this, we choose values for $\epsilon(t+h)$, which do not violate this constraint and which translates the decision maker's choice to a new variable δ. In choosing the constraint dynamically, we expect the conservativeness of the approach to be reduced.

Theorem 4.1 (Feasible minimum value for f_2^j): Consider that at time t, the robot has detected the victim j, which is

described by $\theta_t^j \sim \mathcal{N}\left(\mu_t^j, \Sigma_t^j\right)$. The optimal trajectory that minimizes f_2^j is given by the spiral of Theodorus [25]. The optimal solution $f_2^{j\star}$ for this optimization problem with h time steps later, $\epsilon^j(t+h,t) := \text{minimize } f_2^j(x_{t+1:t+h}|\theta_t^j)$, is obtained as follows

$$
f_2^{j\star} = \text{tr}\left(^g\Sigma_{t+h}^{j\star}\right) = \left(^g\Sigma_t^{j-1} + \sum_{i=t+1}^{t+h} \mathbf{R}(\beta_i^{j\star})^T \Sigma_t^{\text{obs}-1} \mathbf{R}(\beta_i^{j\star})\right)^{-1}
$$

where $\beta_i^{j\star}$ is the sensing angle of the victim in the global coordinate, computed by $\beta_i^{j\star} = \beta_{i-1}^{j\star} - \arcsin\left(\frac{r}{d_{i-1}^j}\right), \ i = t+1, \ldots, t+h$, and $d_i^j = \sqrt{(d_{i-1}^j)^2 - (r)^2}, \ i = t+1, \ldots, t+h$, is the distance between the robot and the victim j with the initial value $d_t^j = \|x_t - \mu_t^j\|$.

Remark 4.1 (Validity of Theorem 4.1): As proved in the theorem above, $\text{tr}(^g\Sigma_{t+h}^j)$ achieves the minimum when $\det(\Xi)$ has its maximum, which is obtained under the assumption that $s_{x|t} > s_{y|t}$. Once this assumption is violated (e.g., $s_{x|t} = s_{y|t}$), $\det(\Xi)$ becomes independent of the choice of β_i^j and for any angle β_i^j, the optimal solution that minimizes $\text{tr}(^g\Sigma_{t+h}^j)$ is obtained. $\bullet$

From the definition of F_2 in (7) with the result in Theorem 4.1, it can be shown that F_2 is lower bounded by $\frac{1}{N}\sum_{j=1}^N \epsilon^j(t+h,t) \leq F_2$, therefore, in order for the multi-objective optimization problem to be feasible, we need to impose that $\epsilon > \alpha \frac{1}{N}\sum_{j=1}^N \epsilon^j(t+h,t)$. Since this should work for any $\alpha \in [0,1]$, and by introducing a constant $\delta > 0$, we transform the right-hand side of our constraint, $\epsilon(t+h)$ in (11) as

$$
\epsilon(t+h) = \tfrac{1}{N}\sum_{j=1}^N \epsilon^j(t+h,t) + \delta,
\tag{12}
$$

with the aim of obtaining a less conservative result with respect to F_2.

The values of δ and α in (11) now control the tradeoffs between F_1, F_3, and F_2 while respecting feasibility. In this way, a choice of α represents a tradeoff between approaching the estimated victim's location and the exploration of the environment. As the value of δ becomes larger, the robot trajectory becomes closer to a straight line between the robot position and the mean location of the victim. This is because the uncertainty constraint about the victim location is relaxed for large δ. However, a small δ is in favor of F_2 objective, making the robot detour around the victim location. For a fixed α, smaller δ may also further increase the chance of finding another victim, which favors the objective xF_3.

B. Planning via Multi-Objective Optimization

We describe the general framework in Algorithm 1 that provides the formal procedure to generate the optimal trajectory of the robot. The proposed dynamic ϵ-constraint method is used at each time step after updating θ_t^j by (3).

If the robot detects victim j, who was not previously found, then increase the total number of detected victims $N \in \mathbb{N}$, followed by the mean $^g\mu_t^j$ and covariance $^g\Sigma_t^j$ update from (3). If $N = 0$ at the current time step t, the weight α is set to be 0. In this stage, the multi-objective optimization problem (11) becomes a F_3 minimization problem

Algorithm 1 Planning via multi-objective optimization

1: initialize $t \leftarrow 0$, $N \leftarrow 0$
2: **while** $\phi(t) > \varepsilon^{\text{stop}}$ **do**
3:    **if** the victim j is detected and j is not visited **then**
4:       **if** j is a new victim **then**
5:          $N \leftarrow N + 1$
6:       **end if**
7:       update $({}^{g}\mu_t^j, {}^{g}\Sigma_t^j)$ from (3)
8:    **end if**
9:    **if** $N = 0$ **then**
10:      $\alpha \leftarrow 0$
11:    **else**
12:      $\alpha \leftarrow 1$
13:      Compute $\epsilon(t + h)$ in (12)
14:    **end if**
15:    Compute $x_{t+1:t+h}$ by solving (11)
16:    Move to x_{t+1}
17:    **if** $\|x_{t+1} - {}^{g}\mu_t^j\| < \varepsilon^{\text{visited}}$ **then**
18:      Mark j as visited
19:      $N \leftarrow N - 1$
20:    **end if**
21:    $t \leftarrow t + 1$
22: **end while**

---

alone. The solution of this optimization problem provides an optimal trajectory $x_{t+1:t+h}$ to minimize the gap between ρ and c_k. If $N > 0$, the weight α becomes 1 and the ϵ value for the dynamic ϵ-constraint method is computed from (12). The optimal trajectory $x_{t+1:t+h}$ is then calculated by solving this ϵ-constraint optimization problem.

If the robot arrives at the location of the victim j, which is determined by the condition $\|x_{t+1} - {}^{g}\mu_t^j\| < \varepsilon^{\text{visited}}$ with a given tolerance value $\varepsilon^{\text{visited}}$, the index j is marked as visited and N is updated by $N \leftarrow N - 1$. Once the robot has visited all locations of currently detected victims, N becomes 0 and α is set to be 0 again. During the ergodic metric computation, the previous trajectory $x_{0:t-1}$ along which the robot has moved is taken into account by the term $c_k(t)$ in (9) and, hence, the optimal trajectory obtained by minimizing F_3 provides the solution to make the robot move to areas which are not explored yet. The robot follows this strategy until the ergodic metric $\phi(t)$ satisfies the terminal condition $\phi(t) \leq \varepsilon^{\text{stop}}$, where $\varepsilon^{\text{stop}}$ is a value provided by the decision maker. covered by the robot.

V. SIMULATIONS

In this section, we present simulations to validate the effectiveness of the proposed multi-objective optimization approach in searching and rescuing victims. The parameter specifications for these two scenarios are given as follows:

1) the measurement range limit: $10\ m$,
2) the maximum moving robot distance per step: $1\ m$,
3) the horizon length: 2,
4) the domain size: $[0, 80] \times [0, 80]\ m^2$
5) the number of victims: 40
6) the sensor noise covariance:

$$\Sigma_t^{\text{obs}} = \begin{bmatrix} 2^2 & 0 \\ 0 & 0.3^2 \end{bmatrix}$$

7) uncertainty tolerance: $\delta = 0.1$, $\forall j = 1, 2, \ldots, 40$.

Throughout simulations, it is assumed that the robot completes its service (e.g., guide and rescue the victim) when the robot arrives at the victim location.

Although the proposed algorithm can be applied to any distributions for $\rho(x)$, we consider that no partial information about the disaster site is given initially and thus, the distribution $\rho(x)$ is assumed to be uniform. Starting from the initial position $[0, 0]^T$, depicted by the cross symbol in Fig. 2 (a), the location of the robot and the sensing range are described by a triangle symbol and a disk, respectively. The square symbols show a found victim. According to the general framework (Algorithm 1), the robot explores the domain uniformly by solving (11) with $\alpha = 0$, since no victims are detected initially.

Whenever the robot detects a possible location of the victim, the weight α changes to 1 and the optimal trajectory is obtained with the dynamic ϵ-constraint. For example, Fig. 2 (b)-(f) show the trajectory along which the robot has moved in the region A of Fig. 2 (a) at different time steps. In these figures, the solid line with circle symbols denotes the planned trajectory up to the given receding horizon length and Arabic numbers represent the detected victims in order. The ellipse describes the uncertainty about the location of the victim. In Fig. 2 (c), the robot detected a new victim (victim #3) while it was approaching the victim #2. This resulted in an increase of F_2 and $\epsilon(t + h)$ was updated by (12) accordingly. The optimizer provides a new trajectory as shown in Fig 2 (d), which detours around the victim #3, in order to satisfy the given constraint for F_2. Fig. 2 (d) presents the same behavior when the robot detected the victim #4. It is interesting to see that in Fig. 2 (d) the robot was heading straight for the victim #1. However, the victim #2 becomes closer and less uncertain as well than any other detected victims while the robot took a detour around the victim #4 after detecting the victim #4 and thus, the robot visited the victim #2 first as shown in Fig. 2 (e). When the robot arrived at the location of the victim #4, no further victims are detected and the weight α becomes 0 again according to Algorithm 1. This strategy is maintained throughout the simulation, which explains the roundabout trajectory of the robot.

VI. CONCLUSIONS

This paper studies a multi-objective optimization problem for disaster response scenarios consisting of objective functions defined by performance, uncertainty about victim locations, and environment uncertainty. Our multi-objective optimization problem formulation combines the weighted-sum and ϵ-constraint method. We adopt a receding-horizon-based algorithm to include new measurement updates at each time step. To deal with the feasibility of the ϵ constraint, we study the optimality of the uncertainty of victims' location along robot trajectories. A formal algorithm is then provided to implement the developed multi-objective optimization approach in the search and rescue task. Future research will focus on the analysis of the Pareto front to take advantage of synergies that arise during the execution for different objectives and scenarios with multiple robots with the assignment

(a) The trajectory of the robot   (b) Zoom-in for the window A at $t = 8$ (c) Zoom-in for the window A at $t = 20$

(d) Zoom-in for the window A at $t = 28$ (e) Zoom-in for the window A at $t = 43$ (f) Zoom-in for the window A at $t = 49$
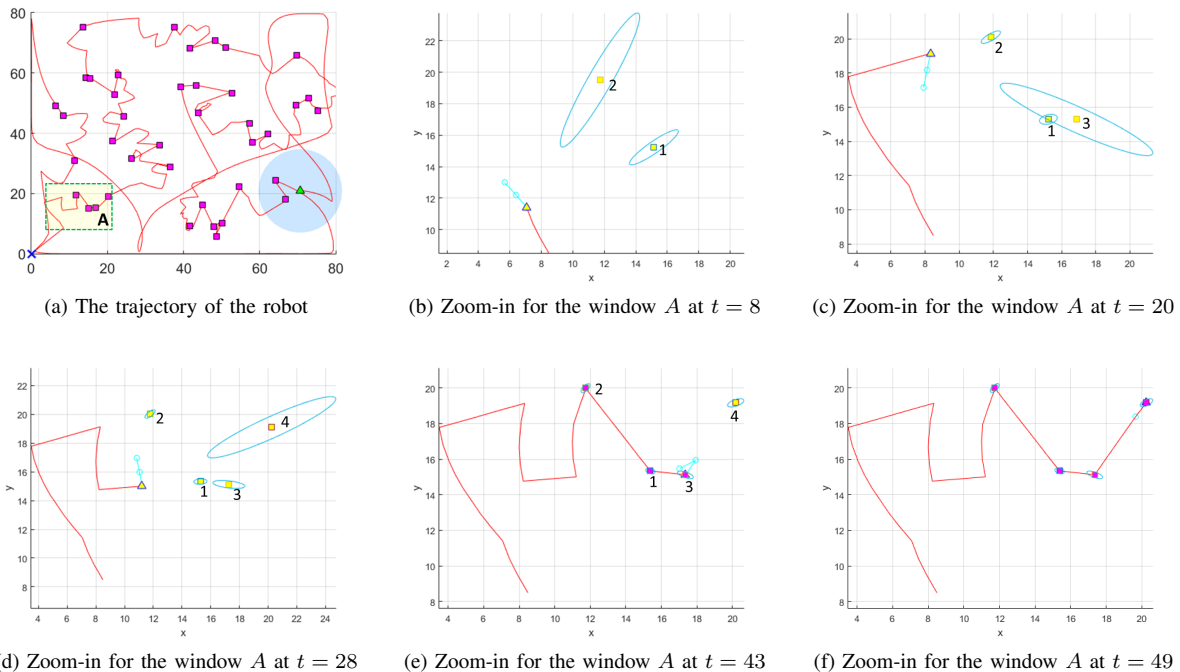
Fig. 2: Simulation results for a search and rescue mission in a disaster response scenario with uniform distribution $\rho(x)$.

of subareas and multiple victims to different agents.

REFERENCES

[1] J. S. Jennings, G. Whelan, and W. F. Evans, "Cooperative search and rescue with a team of mobile robots," in *Advanced Robotics, 1997. ICAR'97. Proceedings., 8th International Conference on*. IEEE, 1997, pp. 193–200.

[2] J. Casper and R. R. Murphy, "Human-robot interactions during the robot-assisted urban search and rescue response at the world trade center," *IEEE Transactions on Systems, Man, and Cybernetics, Part B (Cybernetics)*, vol. 33, no. 3, pp. 367–385, 2003.

[3] T. Tomic, K. Schmid, P. Lutz, A. Domel, M. Kassecker, E. Mair, I. L. Grixa, F. Ruess, M. Suppa, and D. Burschka, "Toward a fully autonomous UAV: Research platform for indoor and outdoor urban search and rescue," *IEEE Robotics & Automation Magazine*, vol. 19, no. 3, pp. 46–56, 2012.

[4] W. Meng, Z. He, R. Teo, R. Su, and L. Xie, "Integrated multi-agent system framework: decentralised search, tasking and tracking," *IET Control Theory & Applications*, vol. 9, no. 3, pp. 493–502, 2014.

[5] E. Galceran and M. Carreras, "A survey on coverage path planning for robotics," *Robotics and Autonomous Systems*, vol. 61, no. 12, pp. 1258–1276, 2013.

[6] Z. L. Cao, Y. Huang, and E. L. Hall, "Region filling operations with random obstacle avoidance for mobile robots," *Journal of Field Robotics*, vol. 5, no. 2, pp. 87–102, 1988.

[7] M. Bosse, N. Nourani-Vatani, and J. Roberts, "Coverage algorithms for an under-actuated car-like vehicle in an uncertain environment," in *Robotics and Automation, 2007 IEEE International Conference on*. IEEE, 2007, pp. 698–703.

[8] F. Yasutomi, M. Yamada, and K. Tsukamoto, "Cleaning robot control," in *Robotics and Automation, 1988. Proceedings., 1988 IEEE International Conference on*. IEEE, 1988, pp. 1839–1841.

[9] S. Hert, S. Tiwari, and V. Lumelsky, "A terrain-covering algorithm for an AUV," *Autonomous Robots*, vol. 3, no. 2, pp. 91–119, 1996.

[10] A. Barrientos, J. Colorado, J. d. Cerro, A. Martinez, C. Rossi, D. Sanz, and J. Valente, "Aerial remote sensing in agriculture: A practical approach to area coverage and path planning for fleets of mini aerial robots," *Journal of Field Robotics*, vol. 28, no. 5, pp. 667–689, 2011.

[11] M. Ollis and A. Stentz, "First results in vision-based crop line tracking," in *Robotics and Automation, 1996. Proceedings., 1996 IEEE International Conference on*, vol. 1. IEEE, 1996, pp. 951–956.

[12] H. Choset, "Coverage for robotics–a survey of recent results," *Annals of mathematics and artificial intelligence*, vol. 31, no. 1, pp. 113–126, 2001.

[13] K. Deb, "Multi-objective optimization," in *Search Methodologies*. Springer, 2014, pp. 403–449.

[14] R. Marler and J. Arora, "Survey of multi-objective optimization methods for engineering," *Structural and Multidisciplinary Optimization*, vol. 26, no. 6, pp. 369–395, 2004.

[15] J. Cohon, *Multiobjective Programming and Planning*. Courier Corporation, 2013.

[16] Y. Ma, Y. Tian, and W. Hou, "Dynamic path optimization of emergency transport based on hierarchical genetic algorithm," *Advances in Swarm Intelligence*, pp. 445–452, 2010.

[17] Y.-H. Lin, R. Batta, P. A. Rogerson, A. Blatt, and M. Flanigan, "A logistics model for emergency supply of critical items in the aftermath of a disaster," *Socio-Economic Planning Sciences*, vol. 45, no. 4, pp. 132–145, 2011.

[18] J. Zhang, J. Peng, Z. Xu, and W. Xu, "SDVRP model for emergency logistics and evolutionary heuristic approach," 2012.

[19] M. Hamedi, A. Haghani, and S. Yang, "Reliable transportation of humanitarian supplies in disaster response: model and heuristic," *Procedia-Social and Behavioral Sciences*, vol. 54, pp. 1205–1219, 2012.

[20] Y. Liu, X. Lai, and G.-L. Chang, "Two-level integrated optimization system for planning of emergency evacuation," *Journal of transportation Engineering*, vol. 132, no. 10, pp. 800–807, 2006.

[21] M. Saadatseresht, A. Mansourian, and M. Taleai, "Evacuation planning using multiobjective evolutionary optimization approach," *European Journal of Operational Research*, vol. 198, no. 1, pp. 305–314, 2009.

[22] M. Defoort, A. Kokosy, T. Floquet, W. Perruquetti, and J. Palos, "Motion planning for cooperative unicycle-type mobile robots with limited sensing ranges: A distributed receding horizon approach," *Robotics and Autonomous Systems*, vol. 57, no. 11, pp. 1094–1106, 2009.

[23] J. M. Mendes-Filho, E. Lucet, and D. Filliat, "Real-time distributed receding horizon motion planning and control for mobile multi-robot dynamic systems," Singapore, Singapore, 2017, pp. 657–663.

[24] G. Mathew and I. Mezić, "Metrics for ergodicity and design of ergodic dynamics for multi-agent systems," *Physica D: Nonlinear Phenomena*, vol. 240, no. 4, pp. 432–442, 2011.

[25] P. J. Davis, W. Gautschi, and A. Iserles, *Spirals: From Theodorus To Chaos*. AK Peters Ltd, 1993.